

# **Some expected extraordinary behaviours of nitride vertical-cavity surface-emitting lasers following from special features of nitride materials**

WŁODZIMIERZ NAKWASKI<sup>1,2</sup>, PAWEŁ MAĆKOWIAK<sup>1</sup>, ROBERT P. SARZAŁA<sup>1</sup>, MICHAŁ WASIAK<sup>1</sup>

<sup>1</sup>Institute of Physics, Technical University of Łódź, ul. Wólczańska 219, 93-005 Łódź, Poland,  
e-mail: nakwaski@p.lodz.pl

<sup>2</sup>Center for High Technology Materials, University of New Mexico, 1313 Goddard SE,  
Albuquerque, NM 87106, USA

In spite of dramatic efforts of numerous technological centres in the world, until now room-temperature continuous-wave operation of nitride diode vertical-cavity surface-emitting lasers (VCSEL) has not been reported. It is probably associated with special features of nitride materials, which essentially distinguish them from other A<sup>III</sup>B<sup>V</sup> semiconductors. In this situation, technological centres need theoretical support to successfully design, modify and optimise possible structures of nitride VCSELs. Therefore, in the present paper, important mutual interactions between physical phenomena taking place inside nitride VCSELs and crucial for their operation are analysed. Some practical guidelines for nitride VCSEL designers are also drawn up.

Keywords: modelling, nitride VCSELs, interactions between physical phenomena.

## **1. Introduction**

Nitrides are very promising new A<sup>III</sup>B<sup>V</sup> semiconductor materials offering some special features which may be useful in manufacturing new optoelectronic devices of performance characteristics unachievable in currently known devices. However, their technology is often very difficult and expensive and their operation characteristics are sometimes far from our expectation.

Nevertheless, there exists nowadays a strong interest in nitride light emitting devices, especially nitride diode lasers, operating in the visible to ultraviolet range of the optical spectrum [1]. In particular, nitride diode vertical-cavity surface-emitting lasers (VCSELs) are very promising candidates for high-density optical storage instruments, underwater communication systems and full-colour displays, to name the most important possible applications. However, there are numerous special features of nitride materials, which essentially distinguish them from other A<sup>III</sup>B<sup>V</sup> semiconductors. In particular, nitride devices exhibit very high room-temperature (RT)

electrical resistivities of *p*-type nitride layers, extremely high electrical resistivities of available (dielectric or semiconductor) distributed-Bragg-reflector (DBR) mirrors, very high electrical *p*-side contact resistivities, carrier-concentration dependent thermal conductivity of nitride layers, lower refractive indices of active-region quantum wells (QWs) than those of barriers, extremely strong spontaneous and stress-related piezoelectric effect as well as very high values of temperature derivatives of nitride indices of refraction. Therefore, not surprisingly, physics of nitride VCSELs differs significantly from that of VCSELs manufactured from other A<sup>III</sup>B<sup>V</sup> semiconductors. Unfortunately, as a result, RT continuous-wave (CW) operation of nitride diode VCSELs has not been reported until now in spite of dramatic and desperate efforts (stimulated by various possible applications of those devices) of numerous technological centres in the world.

Currently, there are two most important problems waiting for a successful solution in possible nitride VCSELs to enable their RT CW operation. While the first one is connected with designing efficient current injection into their active regions, the second one concerns efficiency of radial optical confinement in their cavities. Both problems should be first analysed theoretically, because technological trial and error methods followed by experimental testing are too expensive and time-consuming. Therefore, in this paper, comprehensive self-consistent optical-electrical-gain-thermal three-dimensional modeling of nitride VCSELs is used to simulate precisely their RT CW operation. In particular, important mutual interactions between individual physical phenomena taking place within volumes of nitride VCSELs and crucial for their RT CW operation are analysed and their impact on expected VCSEL performance characteristics is discussed. Some practical guidelines for nitride VCSEL designers are also drawn up.

## 2. Model

The operation of diode lasers is based on mutual interactions of many physical phenomena taking place within their volumes, mostly optical, electrical, recombination, and thermal ones. Therefore, our comprehensive physical model of the operation of nitride VCSELs consists of four mutually interrelated parts: optical, electrical, gain, and thermal ones.

The optical part is based on the effective frequency method [2]. Optical properties of each structure layer as well as possible gain or absorption processes within them are described by 3D profiles of both parts (real and imaginary) of their complex indices of refraction, strictly related not only to a device structure but also to current 3D profiles of temperature and carrier concentration. Lasing threshold is determined, for each radiation mode, from the condition of its real propagation constant.

The electrical part utilizes finite-element (FE) current spreading analysis based on self-consistent solving of the Laplace equation in all individual layers (taking into account 3D profile of composition- and temperature-dependent electrical resistivity) of the laser structure with the exception of an active region, where experimental

current-voltage junction characteristic [3] is used. Radial carrier diffusion within all QWs of an active region is taken into account, including monomolecular nonradiative and Auger recombinations.

Gain spectra are determined using the classical Fermi's golden rule and parabolic band-gap approximation.

The thermal part utilizes the same mesh as the one generated for the electrical calculations and is also based on a FE approach. All important heat sources, including nonradiative recombination, absorption of radiation, as well as barrier and volume Joule heating, are taken into consideration. 3D heat spreading within a laser heat-sink is included. Heat abstraction through the side and the top walls (thermal radiation and thermal convection of air particles) as well as through the top supply wire is neglected because of the much more intense heat conduction through the bottom contact to the device heat sink.

In the simulation, all important interactions between individual physical phenomena are considered, including composition, temperature and carrier-concentration dependences of refractive indices [4]–[8], optical absorption [4], thermal conductivities [9], and electrical resistivities [10]–[12]. The model does not, however, account for piezoelectric built-in fields as high carrier concentrations required to achieve RT CW lasing thresholds in nitride VCSELs effectively screen them [13]. Bandfilling and Coulomb enhancement phenomena [14] are taken into account. A more detailed description of the approach (with all formulae) can be found with some other simulation results in [15]–[27] and general principles of 3D comprehensive VCSEL modelling – in [28].

### 3. Temperature-enhanced current spreading

Because of very high electrical resistivities of all currently available materials for DBR mirrors, a nitride VCSEL should have an annular-contacted structure. Then its central active region is supplied with a current flowing from the upper  $p$ -side contact in a radial direction within the upper  $p$ -type layer (Fig. 1). Therefore, the electrical conductivity of this layer plays an essential role in current-spreading phenomena within the device. Basically, electrical conductivities of semiconductor materials  $\sigma$  are directly proportional to both carrier concentrations and their mobilities. At and above RT, usually most dopants are already ionised because they are chosen to have relatively low activation energies. Therefore, carrier concentrations in standard extrinsic semiconductors are in that case practically independent of temperature. Then, an increase in temperature is followed by a slow decrease in electrical conductivity because of decreasing carrier mobilities. This is standard behaviour of almost all technologically interesting A<sup>III</sup>B<sup>V</sup> materials. With one essential exception – the  $p$ -type nitride materials.

From the very beginning, the  $p$ -type doping of nitride materials has been one of the most severe obstacles to using nitride materials in optoelectronics. Eventually, magnesium dopant was found to create acceptors when a specific treatment is applied.

Nevertheless, the activation energy of the Mg acceptor ( $E_A = 153.54$  meV [10]) has happened to be very high.

Let us consider the test structure of the nitride VCSEL schematically depicted in Fig. 1. The VCSEL has been intentionally designed to emit higher-order transverse modes. Typical values of construction parameters used in the calculations are the following:  $r_1 = 5$   $\mu\text{m}$ ,  $r_2 = 10$   $\mu\text{m}$ ,  $r_3 = 250$   $\mu\text{m}$ ,  $d_p = d_n = 1$   $\mu\text{m}$ ,  $\sigma_p(300\text{K}) = 381$  ( $\Omega\text{m}$ )<sup>-1</sup>,  $\sigma_n(300\text{K}) = 391$  ( $\Omega\text{m}$ )<sup>-1</sup>,  $N_A = 1.48 \times 10^{19}$  cm<sup>-3</sup>,  $N_D = 2 \times 10^{19}$  cm<sup>-3</sup> [11], [12].

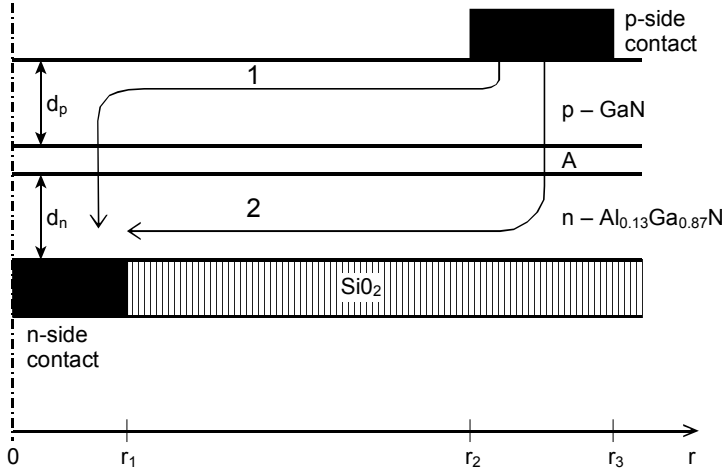
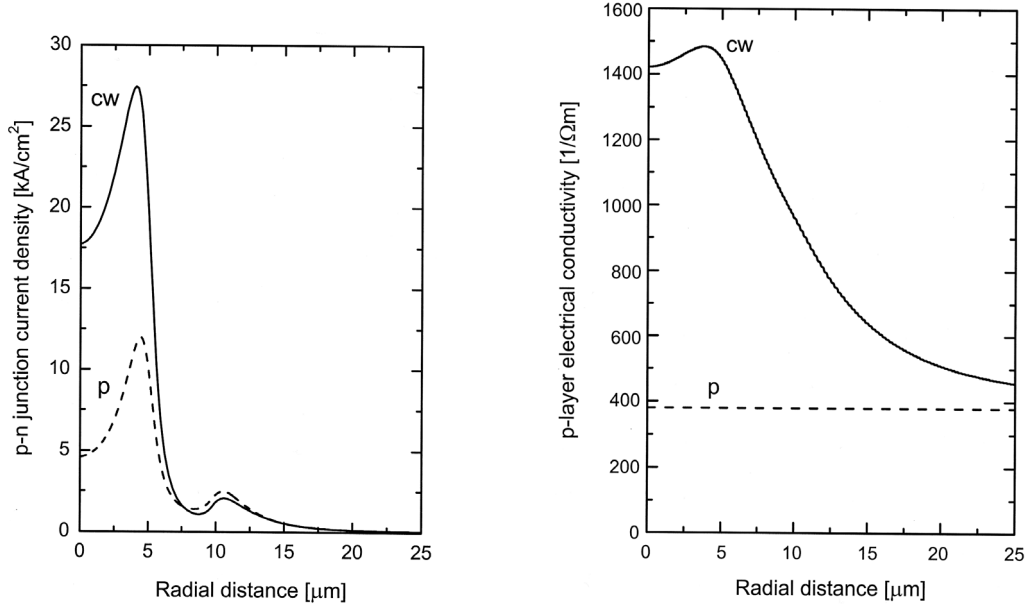


Fig. 1. Schematic view of a test annular-contacted nitride VCSEL structure under consideration. The current spreading is assumed to take place between the annular  $p$ -side contact and the central dot  $n$ -side contact. Two competing current paths are shown: 1 – the current flow supplying the central active region with carriers, and 2 – the unwanted current flow. The VCSEL structure is intentionally designed for higher-order transverse modes.

For the pulse and the CW RT VCSEL operations, radial  $p$ - $n$  junction current density profiles are shown in Fig. 2 labelled as “p” curves and “cw” curves, respectively. Current cross-sections are directly proportional to the radial distance from the structure axis. Therefore, as is clearly seen from Fig. 2, for the pulse operation, a considerable amount (72%) of the total current is in this case crossing the  $p$ - $n$  junction outside the  $r < r_1$  active region. Only the current of 7 mA (of the total 25 mA) is injected into the active region. This current is dramatically increased to as much as almost 19 mA (*i.e.*, by 170%) of the total 38 mA determined for the analogous CW RT case. It is interesting to note that the series electrical resistance of the device is at the same time decreased from 399  $\Omega$  for the RT pulse operation to only 262  $\Omega$  for the CW one.

The reason for the above behaviour may be explained by a radial profile (Fig. 3) of a temperature-dependent electrical conductivity  $\sigma_p$  of the upper  $p$ -type GaN layer. With an increase in temperature, this conductivity is dramatically increased because



▲ Fig. 2. Profiles of the RT  $p$ - $n$  junction current density determined for the nitride VCSEL biased with 10 V: p – pulse and cw – CW operations, respectively.

Fig. 3. Radial profiles along the centre of the  $p$ -type GaN layer of the electrical conductivity  $\sigma_p$  in the nitride VCSEL biased at RT with 10 V: p – pulse and cw – CW operations, respectively.

of a considerable increase in carrier concentrations. Calculated isotherms indicate the annular region of the highest temperature ( $> 415$  K) within just a perimeter area of the active region. Therefore, in spite of a slight decrease in hole mobilities, the conductivity of the  $p$ -type GaN layer is considerably improved in this region (Fig. 3): from  $381 (\Omega\text{m})^{-1}$  for the RT pulse operation to as much as  $1480 (\Omega\text{m})^{-1}$  for the CW one, *i.e.*, by almost 290%. That is why the radial current flow (current 1) towards the central active region before crossing the  $p$ - $n$  junction is distinctly enhanced in the CW-operating nitride VCSELs as compared with pulse-operating ones. The above improves considerably the uniformity of carrier injection into central active regions of possible annular-contacted RT CW-operating nitride VCSELs.

#### 4. Nitride VCSELs intentionally designed for higher-order transverse modes

In the above section, the uniformity of carrier injection into active regions of nitride VCSELs has been found to be drastically improved in CW-operated devices as compared with pulse-operated ones because of the thermally enhanced current-spreading

effect. However, it has been found that, in order to achieve the RT CW VCSEL threshold operation, not only the uniformity of the active-region carrier concentration considered above but also that of temperature distribution within the VCSEL active region neighbourhood are equally important. Besides, mostly because of the problems with effective confinement of an optical field in a radial direction, RT CW lasing in nitride VCSELs is usually easier to achieve on higher-order transverse modes than on lower-order ones. Therefore, a novel VCSEL design with an additional central dot  $p$ -side contact (see, *e.g.*, Fig. 1) has been intentionally created to enhance the excitation of low-threshold high-order transverse modes.

In all structures of nitride VCSELs under consideration, 4 pairs of the dielectric  $\text{SiO}_2/\text{TiO}_2$  DBR are used as an upper resonator mirror and 24 pairs of the semiconductor high-thermal-conductivity  $\text{AlN}/\text{Al}_{0.15}\text{Ga}_{0.85}\text{N}$  DBR are applied on the bottom side of the structure to additionally ensure efficient heat extraction, which is important in the case of the CW operation. The layers between the bottom and the top DBR resonator mirrors comprise the  $3\text{-}\lambda$  cavity. The desired emission wavelength is assumed to be 400 nm. A more detailed analysis of the most suitable DBR configuration for nitride VCSELs can be found in [23]. Spacer thicknesses have been optimised to achieve the lowest threshold gain.

The number of QWs is limited to 5 due to a possible interwell inhomogeneity of carrier injection [29]. For the same reasons, a 10% gain drop in successive QWs is assumed [30]. The active region is postulated to be the one analysed by PARK and CHUANG [31], so it is composed of  $\text{In}_{0.15}\text{Ga}_{0.85}\text{N}$  QWs separated by  $\text{In}_{0.02}\text{Ga}_{0.98}\text{N}$  barriers.

A typical double-ring-contacted (RC) VCSEL structure utilizes a classical double lateral current injection. Its  $n$ -side and  $p$ -side ring contacts are separated by high resistive regions beyond the central device part which (together with the temperature distribution considered earlier in Sec. 3) enhances radial current flow from the upper ring contact towards the laser axis, *i.e.*, to the central laser part containing its active region.

The second design considered, the double-contacted (DC) VCSEL, evolved from the first one. Its both intra-cavity annular contacts are preserved. However, an additional dot-like  $p$ -side contact is placed in the centre of the structure and an additional high-resistivity region is created over it. It has been found that the dot-like contact is very important to enhance the uniformity of current density injection into the active region. We have modelled two versions of the DC VCSEL structure: the first one (DC-A VCSEL) has longer the dot-like contact radius (3  $\mu\text{m}$ ) than the second one (DC-B VCSEL – 2  $\mu\text{m}$ ).

Most performance properties of traditional RC nitride VCSELs follow from the extremely nonuniform current injection into their active regions, which has already been discussed in this work and which is shown in Fig. 4. As one can see, in this case, the current injection through the  $p$ - $n$  junction is practically confined to a narrow ring close to the active-region edge. Hardly any current reaches the device axis. It is

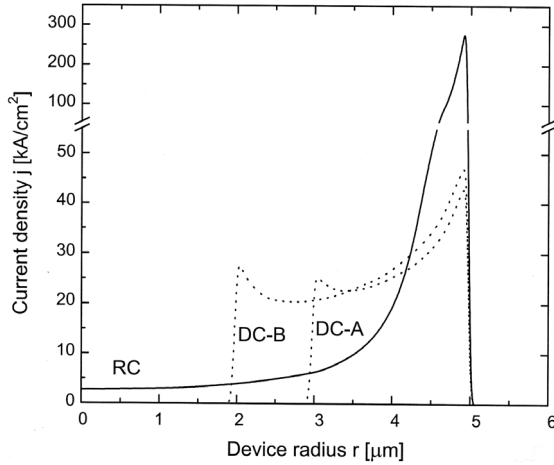


Fig. 4. Radial distributions of the  $p$ - $n$  junction current density in modelled VCSEL devices determined for the operation currents slightly exceeding their RT CW threshold values. Note the condensed scale at the top of the figure.

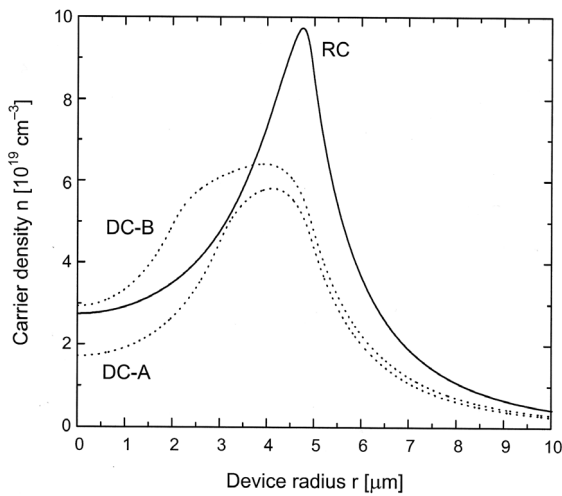


Fig. 5. Radial distributions of the active-region carrier concentration in modelled VCSEL devices determined for the operation currents slightly exceeding their RT CW threshold values.

followed by a still very nonuniform profile of active-region carrier concentration (Fig. 5) and by proportional to it an optical gain. This situation strongly favours excitation of higher-order transverse modes [24]. Therefore, the first mode to be excited at lasing RT CW threshold is the very-high-order  $LP_{22,1}$  mode. Besides, radial profiles of many various  $LP_{L,1}$  modes ( $L = 0, 1, 2, \dots$ ) are practically indistinguishable

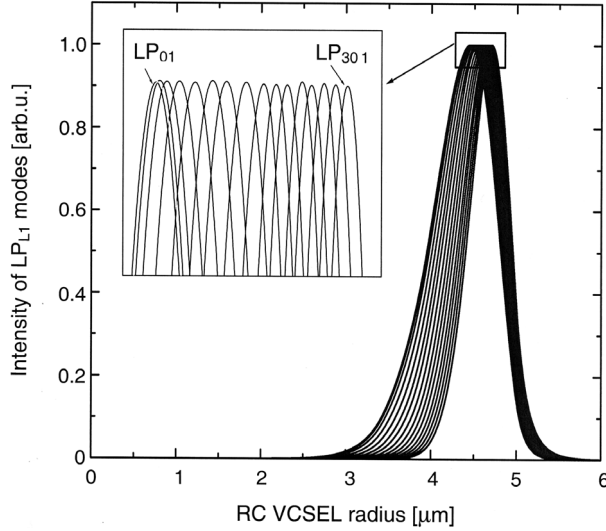


Fig. 6. Radial intensity profiles of the  $LP_{L1}$  transverse modes in the modelled RC VCSEL. Note that the active region extends in this laser from the symmetry axis to the  $5 \mu\text{m}$  radius, whereas all the  $LP_{L1}$  transverse modes occupy practically only the area close to the active-region perimeter.

from one another (Fig. 6) which is followed by very similar (practically the same) RT CW threshold values of their modal gains and, consequently, by an unavoidable multimode RT CW operation of this laser.

## 5. Thermal focusing

RT CW lasing thresholds of successive modes are in the RC laser relatively high and very similar to one another not only because of poor overlapping between their mode intensity profiles and an optical gain distribution but also as a result of the thermal waveguiding effect. Radial temperature profile determined for the lasing threshold (Fig. 7) has its distinct maximum very close to the active-region perimeter. Hence the thermal focusing is trying to shift an optical field towards the active-region edge. This is followed by an increasing field penetration of passive areas located around the active region, so the overlapping of optical gain distribution and optical field is additionally reduced and modal losses in passive areas are considerably increased. This means that more carriers (that is higher operation currents) are necessary for this mode to reach its lasing threshold and that more higher-order transverse modes exhibit similar RT CW lasing thresholds. So, in nitride VCSELs, uniformity of both the carrier concentration and temperature profiles within their active regions are turned out to be equally important for their mode selectivity. The above effect is known also in other VCSELs, but it is especially important in nitride ones because nitride refractive indices change with an increasing temperature much more rapidly [32] than in other semiconductor materials.



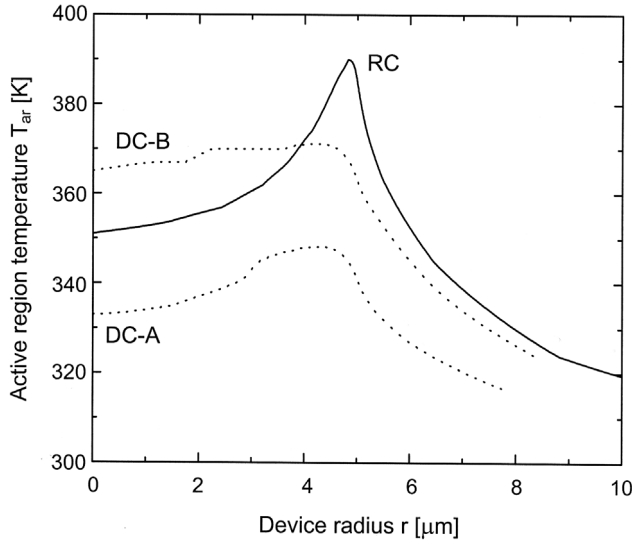


Fig. 7. Radial distributions of the active-region temperature in modelled VCSEL devices determined for the operation currents slightly exceeding their RT CW threshold values.

The inspiration for our design came from the analysis of light intensity radial profiles of the  $LP_{L1}$  modes in a resonator of the RC nitride VCSEL (Fig. 6). Their optical fields are practically confined to a ring area close to the active-region perimeter, leaving its broad central part empty. Therefore, we propose to place there an additional dot  $p$ -side contact and the additional layer of lower conductivity (*e.g.*, GaN slightly doped with Si) above the junction but below the  $n$ -type spacer. We try to shape  $p$ -side contacts to obtain more uniform not only the active-region carrier concentration but also the temperature in the active-region neighbourhood. As one can see in Figs. 4, 5 and 7, performance characteristics of both new DC VCSELs are much closer to optimal ones than those of the RC laser. In particular, both carrier-concentration (Fig. 5) and temperature (Fig. 7) distributions are nearly perfectly uniform within VCSEL active regions. Therefore, transverse modes of much lower (but still quite high) orders have matched gain profiles first: the  $LP_{12\ 1}$  mode (DC-A VCSEL) and the  $LP_{7\ 1}$  mode (DC-B VCSEL) *vs.* the  $LP_{22\ 1}$  mode in the case of the RC laser. Besides, much lower modal gain is necessary to reach RT CW thresholds:  $23.6\ \text{cm}^{-1}$  (DC-A VCSEL) and  $25.1\ \text{cm}^{-1}$  (DC-B VCSEL) *vs.*  $41.3\ \text{cm}^{-1}$  in the RC laser. As a result, RT CW threshold currents of DC VCSELs are noticeably lower.

## 6. Conclusions

Nitride edge-emitting (EE) diode lasers are already commercially available. However, it is not the nitride EE lasers but the much more complicated technologically nitride VCSELs that are believed to be the most promising structure of nitride diode lasers. But in spite of very promising expected application areas of nitride VCSELs followed

by desperate efforts of many technological centres in the world trying to manufacture their structures, RT CW operation of these devices has not been reported until now. In this situation, technologists need theoretical support in designing new and more suitable nitride VCSEL structures taking into consideration their real material and device properties.

Therefore, in this paper, an advanced 3D optical-electrical-gain-thermal self-consistent model has been used to investigate performance of possible nitride VCSELs followed from some special features of nitride materials and nitride structures and to anticipate performance characteristics of possible designs of nitride VCSELs. In particular, temperature-enhanced radial current spreading in the upper *p*-type layer (being a result of both its extremely low electrical conductivity and its rapid increase with temperature) as well as thermal focusing in the active-region neighbourhood (followed from a very rapid temperature increase in the index of refraction) are found to stimulate, respectively, distinctly more uniform current injection into VCSEL active regions and better radial optical waveguiding within VCSEL cavities. Both the above special features of possible nitride VCSELs, if properly utilized, may enable their first RT CW operation.

*Acknowledgments* – This work was supported by the Polish State Committee for Scientific Research (KBN) under the grant No. T11B 073 21.

## References

- [1] NAKAMURA S., FASOL G., *The Blue Laser Diode*, Springer, Berlin 1997.
- [2] WENZEL H., WÜNSCHE H.J., *IEEE J. Quantum Electron.* **33** (1997), 1156.
- [3] SONG Y.-K., DIAGNE M., ZHOU H., NURMIKKO A.V., SCHNEIDER JR., R.P., TAKEUCHI T., *Appl. Phys. Lett.* **77** (2000), 1744.
- [4] PALIK E.D. [Ed.], *Handbook of Optical Constants of Solids*, Academic Press, Orlando 1985.
- [5] BRUNNER D., ANGERER H., BUSTARRED E., FREUDENBERG F., HOEPLER R., DIMITROV R., AMBACHER O., STUTZMANN M., *J. Appl. Phys.* **82** (1997), 5090.
- [6] MANDY M., LEUNG Y., DJURISIC A.B., LI E.H., *J. Appl. Phys.* **84** (1998), 6312.
- [7] BERGMANN M.J., CASEY, JR., H.C., *J. Appl. Phys.* **84** (1998), 1196.
- [8] JIANG H.X., LIN J.Y., *Appl. Phys. Lett.* **74** (1999), 1066.
- [9] FLORESCU D.I., ASNIN V.A., MOUROKH L.G., POLLAK F.H., MOLNAR R.J., WOOD C.E.C., *J. Appl. Phys.* **88** (2000), 3295.
- [10] TANAKA T., WATANABE A., AMANO H., KOBAYASHI Y., AKASAKI I., YAMAZAKI S., KOIKE M., *Appl. Phys. Lett.* **65** (1994), 593.
- [11] YOSHIDA S., MISAWASA S., GONDA S., *Appl. Phys. Lett.* **53** (1982), 6844.
- [12] GÖTZ W., JOHNSON N.M., CHEN C., LIU H., KUO C., IMLER W., *Appl. Phys. Lett.* **68** (1996), 3144.
- [13] SALA F.D., CARLO A.D., LUGLI P., BERNARDINI F., FIORENTINI V., SCHOLZ R., JANCU J.-M., *Appl. Phys. Lett.* **74** (1999), 2002.
- [14] ZUKAUSKAS A., JURESENAS S., KURLICK G., TAMULAITIS G., SHUR M.S., GASKA R., YANG J.W., KHAN M.A., *Phys. Status Solidi B* **216** (1999), 501.
- [15] MAĆKOWIAK P., NAKWASKI W., *J. Phys. D: Appl. Phys.* **31** (1998), 2479.
- [16] *Ibidem*, *MRS Internet J. Nitride Semicond. Res.* **3** (1998), Article 35.
- [17] *Ibidem*, *Opt. Quantum Electron.* **31** (1999), 1179.
- [18] *Ibidem*, *Opt. Appl.* **30** (2000), 125.

- [19] *Ibidem*, J. Phys. D: Appl. Phys. **33** (2000), 642.
- [20] *Ibidem*, J. Phys. D: Appl. Phys. **34** (2001), 954.
- [21] CZYSZANOWSKI T., NAKWASKI W., J. Phys. D: Appl. Phys. **34** (2001), 1277.
- [22] SARZAŁA R.P., MAĆKOWIAK P., NAKWASKI W., Semicond. Science Technol. **17** (2002), 255.
- [23] MAĆKOWIAK P., NAKWASKI W., Opt. Appl. **32** (2002), 493.
- [24] NAKWASKI W., MAĆKOWIAK P., WASIAK M., SARZAŁA R.P., CZYSZANOWSKI T., Phys. Status Solidi **C 0** (2002), 48.
- [25] MAĆKOWIAK P., SARZAŁA R. P., WASIAK M., NAKWASKI W., IEEE Photon. Techn. Lett. **15** (2003), 495.
- [26] MAĆKOWIAK P., CZYSZANOWSKI T., SARZAŁA R. P., WASIAK M., NAKWASKI W., Opto-Electronics Rev. **11** (2003), 119.
- [27] MAĆKOWIAK P., SARZAŁA R. P., WASIAK M., NAKWASKI W., J. Phys. D: Appl. Phys. **26** (2003) 2041.
- [28] OSIŃSKI M., NAKWASKI W., [Chapter 5 in] *Vertical-Cavity Surface-Emitting Laser Devices* [Eds.] H. Li and K. Iga, Springer, Berlin 2003.
- [29] DOMEN K., SOEJIMA R., KURAMATA A., HORINO K., KUBOTA S., TANAHASHI T., Appl. Phys. Lett. **73** (1998), 2775.
- [30] TESSLER N., EISENSTEIN G., IEEE J. Quantum Electron. **29** (1993), 1586.
- [31] PARK S.-H., CHUANG S.-L., Appl. Phys. Lett. **72** (1998), 287.
- [32] ZHAO G.Y., ISHIKAWA H., EGAWA G.YU.T., WATANABE J., SOGA T., JIMBO T., UMENO M., Appl. Phys. Lett. **73** (1998), 22.

*Received November 5, 2003*